applied sciences

MDPI

Article

Effects of the Concentration of Eu^{3+} Ions and Synthesizing Temperature on the Luminescence Properties of $Sr_{2-x}Eu_xZnMoO_6$ Phosphors

Chi-Yu Lin [1], Su-Hua Yang [2], Jih-Lung Lin [3] and Cheng-Fu Yang [4,*]

1 Department of Aero-Electronic Engineering, Air Force Institute of Technology, Kaohsiung 820, Taiwan, R.O.C.; takiincku@yahoo.com.tw
2 Department of Electronic Engineering, National Kaohsiung University of Applied Sciences, Kaohsiung 807, Taiwan, R.O.C.; shya@cc.kuas.edu.tw
3 Department of Aeronautics and Astronautics, Air Force Academy, Kaohsiung 820, Taiwan, R.O.C.; lin2737.cafa@msa.hinet.net
4 Department of Chemical and Material Engineering, National University of Kaohsiung, Kaohsiung 811, Taiwan, R.O.C.
* Correspondence: cfyang@nuk.edu.tw; Tel.: +886-7-591-9283

Academic Editors: Teen-Hang Meen, Antonio Facchetti and Giorgio Biasiol
Received: 13 September 2016; Accepted: 22 December 2016; Published: 27 December 2016

Abstract: The effect of Eu_2O_3 concentration on the luminescence properties of double perovskite (cubic) $Sr_{2-x}Eu_xZnMoO_6$ phosphors was thoroughly investigated using different synthesizing temperatures. Phosphors with the composition $Sr_{2-x}Eu_xZnMoO_6$, where Eu_2O_3 was substituted for SrO and x was changed from 0 to 0.12, were synthesized by the solid-state method at temperatures of 900–1200 °C, respectively. Analysis of the X-ray diffraction (XRD) patterns showed that even when the synthesizing temperature was 1100 °C, secondary or unknown phases were observed in $Sr_{2-x}Eu_xZnMoO_6$ ceramic powders. The effect of the concentration of Eu^{3+} ions on the luminescence properties of the $Sr_{2-x}Eu_xZnMoO_6$ phosphors was readily observable because no characteristic emission peak was observed in the Sr_2ZnMoO_6 phosphor. Two characteristic emission peaks at 597 and 616 nm were observed, which correspond to the $^5D_0$–$^7F_1$ and $^5D_0$–$^7F_2$ transitions of Eu^{3+} ions, respectively. The two characteristic emission peaks of the $Sr_{2-x}Eu_xZnMoO_6$ phosphors were apparently influenced by the synthesizing temperature and the concentration of Eu^{3+} ions. When x was larger than 0.08, a concentration quenching effect of Eu^{3+} ions in the $Sr_{2-x}Eu_xZnMoO_6$ phosphors could be observed. The lifetime of the $Sr_{2-x}Eu_xZnMoO_6$ phosphors decreased as the synthesizing temperature increased. A linear relation between temperature and lifetime was obtained by using a fitting curve of $t = -0.0016 \times T + 3.543$, where t was lifetime and T was synthesizing temperature.

Keywords: $Sr_{2-x}Eu_xZnMoO_6$ phosphors; double perovskite oxides; synthesizing temperature; lifetime

1. Introduction

UV light can be generated as a consequence of electronic transitions of light sources through an Hg discharge. In low-pressure Hg discharge, the main emission line is located at a wavelength of 254 nm. This light is invisible and harmful to human bodies, so it has to be converted into visible light, which can be done with a combination of luminescent materials. These luminescent materials can strongly absorb light of that wavelength and efficiently convert it into visible light. Recently, white light emitting diodes (LEDs) have become popular because they have several advantages, including high efficiency, long lifetime, and low power consumption. Red phosphors are also helpful for generating

white light when they are excited by blue or near-UV lights. To obtain phosphors with highly efficient emissions, it is important to choose the right compound materials and ensure they have outstanding physical and chemical stability. Numerous studies have explored different luminescent materials to enable the development of suitable phosphors. When lanthanide contraction ions are introduced into host materials, unfilled $4f^N$ electron orbitals result, and these have attracted considerable attention. The resulting phosphors emit very luminescent emissions with specific light wavelengths because of variations in the energy level of some free electrons [1–4]. These phosphors have been the most promising candidates for applications in fluorescent lamps and flat panel display devices, such as electroluminescence panels, plasma display panels, and field emission displays.

A large number of isotropic compounds with perovskite structures, such as double perovskite oxides, have the general formula $A_2BB'O_6$, in which BO_6 and $B'O_6$ octahedra are corner-shared, alternately. The great flexibility of A and $B(B')$ sites in $A_2BB'O_6$ allows very rich substitutions, and this framework forms cube-octahedral cavities filled by A-site cations [5,6]. Double perovskites with the formula $A_2BB'O_6$, where A uses an alkaline earth, B and B' are metal transition magnetic and nonmagnetic ions, and O is oxygen, have been investigated as magnetic materials for many years. For example, Sr_2CrMoO_6 has been studied as a half-metallic system [7]. Kobayashi et al. recently reported room-temperature low-field magnetic resistance in the ordered double perovskite Sr_2FeMoO_6 [8]. Complete ordering of Fe and Mo on the B and B' sites of this metallic $A_2BB'O_6$ double perovskite is predicted to give half-metallic ferromagnetism with localized majority-spin electrons on the Fe atoms [9,10]. Recently, the study of $A_2BB'O_6$-based materials has increased due to various technological applications, such as inorganic oxide luminescent materials.

The emitting materials are usually composed of activators and a host lattice. Some host lattice materials can produce light themselves, and some can produce light when doped with rare-earth activators (ions). Rare-earth ions are known to exist in various valence states, although the trivalent state is the most prevalent. Rare-earth ions can be applied in lighting devices and display panels due to their abundant energy levels across a wide spectrum range, from ultraviolet to near infrared. Sm- and Eu-based ions are the most commonly used dopants because they are stable in trivalent (Sm^{3+} and Eu^{3+}), as well as divalent (Eu^{2+}), states. The luminescence of rare-earth ions doped in perovskite-type ceramics was actively investigated in the 1960s and 1970s because of interest in their ferroelectricity, phase transitions, and semiconducting properties [11]. Recently, many studies have shown that the double perovskite structure with a composition of A_2BMO_6 (A = Ba, Sr; B = Ca, Zn; M = Mo, W) is activated by trivalent europium ions (Eu^{3+}) [12–15]. Phosphors activated by Eu^{3+} are considered ideal red sources because of their sharp emission lines in the red region [12–16]. Eu^{3+}-doped double-perovskite materials have a broad excitation band ranging from UV to visible light, and they also show highly efficient red luminescence. For that, Eu^{3+}-doped double molybdenum (Mo)-based double perovskite oxides have attracted significant attention for their possible application as luminescent materials, such as $Sr_2MgMo_xW_{1-x}O_6$: Eu^{3+} [17], $Sr_2Ca(Mo/W)O_6$: Eu^{3+} [18], Sr_2CaMoO_6: Eu^{3+} [19], $(Ba,Sr)_2CaMoO_6$: Eu^{3+}, Yb^{3+} [20], Ca_2LaMO_6: Eu^{3+} (M = Sb, Nb, Ta) [21], and A_2CaMoO_6 (A = Sr, Ba) [6], respectively.

To the best of our knowledge, the luminescent characteristics of concentrated Eu^{3+} ions in $Sr_{2-x}Eu_xZnMoO_6$ phosphors, which are molybdenum-based double-perovskite oxides, have not been reported. In this study, the red-emitting phosphors of Eu^{3+}-doped Mo-based double-perovskite $Sr_{2-x}Eu_xZnMoO_6$ oxides were synthesized by the conventional high-temperature solid state reaction method. We found that Eu^{3+} concentration and the synthesizing temperature of the $Sr_{2-x}Eu_xZnMoO_6$ phosphors had a large effect on their luminescent characteristics. The concentration quenching effect of Eu^{3+} ions in $Sr_{2-x}Eu_xZnMoO_6$ phosphors was found and would be well discussed [22]. In this study, the first important novelty is that we have not found any similar studies about $Sr_{2-x}Eu_xZnMoO_6$ phosphors. The second important novelty is that we found a linear relationship between the synthesizing temperature and lifetime of $Sr_{2-x}Eu_xZnMoO_6$ phosphors. We also investigated the relationship between the synthesized temperature and lifetime of $Sr_{2-x}Eu_xZnMoO_6$ phosphors.

2. Materials and Methods

$Sr_{2-x}Eu_xZnMoO_6$ powders were synthesized through the solid-state reaction method. Stoichiometric amounts of $SrCO_3$, ZnO, MoO_3, and Eu_2O_3 were weighed according to the composition formula of $(2 - x)$ $SrCO_3$ + ZnO + MoO_3 + $(0.5\ x)$ Eu_2O_3, where x = 0, 0.04, 0.06, 0.08, 0.10, and 0.12, respectively. After being mixed in acetone, dried, and ground, the solid-state reaction method was used to heat the $Sr_{2-x}Eu_xZnMoO_6$ compositions in an air atmosphere. The $Sr_{2-x}Eu_xZnMoO_6$ powders were heated to 900 °C, 1000 °C, 1100 °C, and 1200 °C for 4 h. When the synthesizing temperature was equal to 1300 °C, the $Sr_{2-x}Eu_xZnMoO_6$ was melted and gathered together to not be used as part of the phosphors. The crystalline structures of the synthesized $Sr_{2-x}Eu_xZnMoO_6$ powders were measured using X-ray diffraction (XRD) (Bruker, Boston, MA, USA) patterns with Cu Kα radiation (λ = 1.5418 Å) and with a scanning speed of 2° per minute. Photoluminescence (PL) properties were recorded at room temperature in the wavelength range of 450–800 nm on a Hitachi F-4500 fluorescence spectrophotometer (Hitachi, Tokyo, Japan). In the past, we had found that 271 nm had a better excitation effect on $BaZr_{1-x}Eu_xO_3$ powders [16]. This result suggested that we would also need to find the optimum optical wavelength for exciting the $Sr_{2-x}Eu_xZnMoO_6$ powders. In this study, the three-dimensional (3D) scanning process using a spectrophotometer (Hitach, Tokyo, Japan) was used to find the optimum optical wavelength, and this value was dependent on the compositions of the $Sr_{2-x}Eu_xZnMoO_6$ phosphors and the synthesizing temperature. We found that the optimum exciting optical wavelength for all of the $Sr_{2-x}Eu_xZnMoO_6$ powders was 350 nm, and the $Sr_{2-x}Eu_xZnMoO_6$ powders excited by other wavelengths had the weaker PL intensities.

3. Results and Discussion

To achieve high PL properties, the preparation of $Sr_{2-x}Eu_xZnMoO_6$ powders forming the double-perovskite phase is very important, because crystallization of $Sr_{2-x}Eu_xZnMoO_6$ powders influences their photoluminescent properties. Figure 1 shows the XRD patterns of our $Sr_{2-x}Eu_xZnMoO_6$ powders as a function of the synthesizing temperature. The strong peaks occurred at around 31.9° for the (220) diffraction peak of the six host lattices. Those results suggest that the XRD patterns showed stable double-perovskite features regardless of the synthesizing temperature and Eu^{3+} concentration.

As Figure 1a shows, when the synthesizing temperature of the $Sr_{2-x}Eu_xZnMoO_6$ powders was 900 °C and as the x value increased from 0 to 0.12, the 2θ value of the (220) diffraction peak shifted from 31.85 to 31.87 and the full width at half maximum (FWHM) values for the (220) diffraction peak were in the range of 2θ = 0.25°–0.27°. When the synthesizing temperature was 1200 °C, the 2θ value of the (220) diffraction peak shifted from 31.88 to 31.90, and the FWHM values for the (220) diffraction peak of the $Sr_{2-x}Eu_xZnMoO_6$ powders were in the range of 2θ = 0.19–0.20°, as the x value of the $Sr_{2-x}Eu_xZnMoO_6$ powders increased from 0 to 0.12. The results in Figure 1a–d show that the 2θ of the (220) diffraction peak shifted to a higher value and the FWHM values for the (220) diffraction peaks of the $Sr_{2-x}Eu_xZnMoO_6$ powders decreased as the synthesizing temperature increased.

The ideal cubic double-perovskite structure (with the same space group $Pm\bar{3}m$ (221)) can be described by a faced-centered cubic (fcc) lattice with lattice constant 2a [23]. The $B(B')$ ion is coordinated by the $B'(B)$ ion using an O ion as an intermediate in the middle, and the lengths of B–O and B'–O are considered to be equal. After relaxation, both lattice constants and atomic positions reduce the ideal cubic structure (space group $Fm\bar{3}m$) to a tetragonal structure (space group $I4/mmm$). There are two O_1 atoms located on the z-axis with B and B' atoms sitting between, and the four O_2 atoms are located on the xy-plane; the same as the B and B' atoms. The angle of the B–O–B' remains at 180° during structural optimization, whereas the lattice constant and bond length change. The lattice a can be calculated by using (1) the reflection peaks (011), (111), (200), and (220) from the XRD patterns in Figure 1; and (2) the closeness of the c/a ratio to the ideal value of $\sqrt{2}$. As the synthesizing temperature was 900 °C, the $Sr_{2-x}Eu_xZnMoO_6$ powders exhibited a cubic crystal structure with the cell parameters changing from $a = b = c/\sqrt{2}$ = 0.3968 nm to $a = b = c/\sqrt{2}$ = 0.3971 nm as the concentration of Eu^{3+} ions

increased from 0 to 0.12. The cell parameters for $Sr_{2-x}Eu_xZnMoO_6$ powders synthesized at 1200 °C were also calculated from the XRD patterns shown in Figure 1, and the cell parameters changed from $a = b = c/\sqrt{2} = 0.3971$ nm to $a = b = c/\sqrt{2} = 0.3974$ nm as the concentration of Eu^{3+} ions increased from 0 to 0.12. These results were in good agreement with those from the Joint Committee on Powder Diffraction Standards (JCPDS) file number 742474.

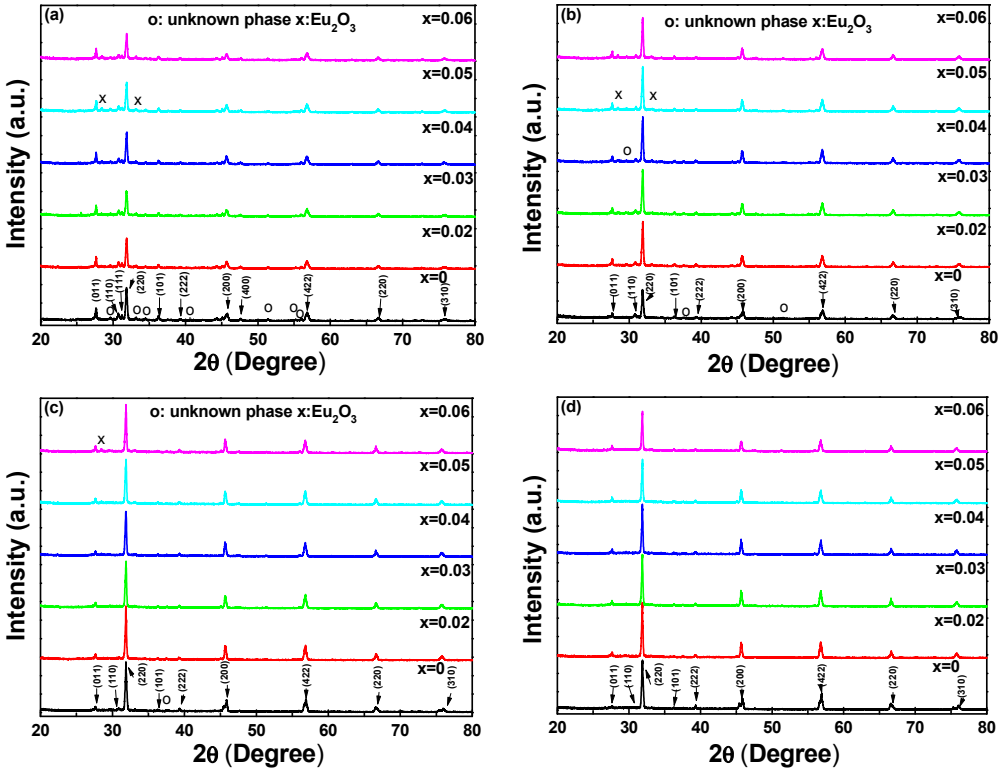

Figure 1. XRD patterns of $Sr_{2-x}Eu_xZnMoO_6$ phosphors synthesized at (**a**) 900 °C; (**b**) 1000 °C; (**c**) 1100 °C; and (**d**) 1200 °C for 4 h, respectively.

As the results of the X-ray diffraction (XRD) patterns showed in Figure 1 were compared, these results indicated that the diffraction intensities of unknown phases for peaks located at around $2\theta = 28.44°$ and 33.09° increased as the concentration of Eu^{3+} ions increased and decreased as the synthesizing temperature increased. Those peaks are in good agreement with the (222) and (400) peaks of JCPDS file number 120393 for cubic Eu_2O_3. The decrease in the diffraction intensities of peaks located at around $2\theta = 28.44°$ and 33.09° prove that more Eu^{3+} ions will substitute the sites of Sr^{2+} ions as the synthesizing temperature is raised. Even when the synthesizing temperature was 1100 °C, secondary or unknown phases were observed in the $Sr_{2-x}Eu_xZnMoO_6$ ceramic powders. These Eu_2O_3 and secondary or unknown phases were not observed when the synthesizing temperature was 1200 °C. These results suggest that when the same synthesizing temperature is used, the concentration of Eu^{3+} ions has no apparent effect on the crystallization of $Sr_{2-x}Eu_xZnMoO_6$ powders; hence, the synthesizing temperature is an important factor in determining the crystalline properties of $Sr_{2-x}Eu_xZnMoO_6$ powders. Additionally, the concentration of Eu^{3+} ions and the synthesizing temperature affect the photoluminescent properties of $Sr_{2-x}Eu_xZnMoO_6$ phosphors.

XRD patterns for $Sr_{2-x}Eu_xZnMoO_6$ phosphors synthesized at 1200 °C for 4 h in the narrow range of 29–35° are shown in Figure 2. These results are significant. Initially, the splitting of the (220) diffraction peak was observed in the Sr_2ZnMoO_6 and $Sr_{1.98}Eu_{0.02}ZnMoO_6$ phosphors, but it was not observed in other $Sr_{2-x}Eu_xZnMoO_6$ phosphors. The two split peaks of the Sr_2ZnMoO_6 phosphors were located at $2\theta = 31.83°$ and 31.88°, and the two split peaks of the $Sr_{1.98}Eu_{0.02}ZnMoO_6$

phosphors were located at 2θ = 31.81° and 31.89°. These results suggest that the Sr_2ZnMoO_6 and $Sr_{1.98}Eu_{0.02}ZnMoO_6$ phosphors revealed a perovskite structure with the tetragonal phase. As the concentration of Eu^{3+} was more than 0.02, the $Sr_{2-x}Eu_xZnMoO_6$ phosphors would have transformed from the tetragonal phase to the (pseudo-)cubic phase, since the splitting of the (220) diffraction peak was not observed. Since the $Sr_{2-x}Eu_xZnMoO_6$ phosphors were tetragonal phase or (pseudo-)cubic phase, even when the concentration of Eu^{3+} ions was increased to 0.12, this result also proves that the Eu^{3+} ions would have substituted into the sites of Ba^{2+} ions. If the Eu^{3+} ions had substituted into the sites of Zn^{2+} (or Mo) ions, the $Sr_{2-x}Eu_xZnMoO_6$ phosphors would have revealed other crystalline phases, or more secondary phases would have been revealed in the $Sr_{2-x}Eu_xZnMoO_6$ phosphors rather than in the double-perovskite features.

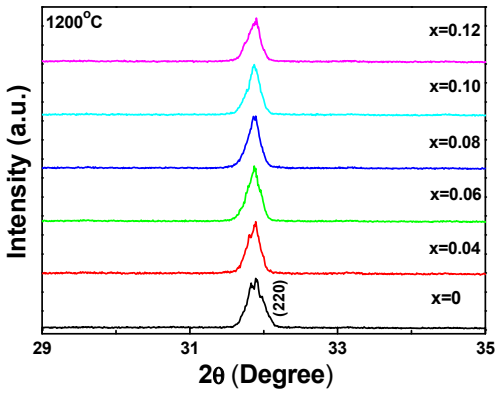

Figure 2. XRD patterns of $Sr_{2-x}Eu_xZnMoO_6$ phosphors synthesized at 1200 °C for 4 h.

Previously, Lin et al. successfully synthesized novel near-UV and blue-excited Eu^{3+}, Tb^{3+}-co-doped one-dimensional strontium germanate full-color nanophosphors by a simple sol-hydrothermal method. They found that incorporation of the Eu^{3+} and Tb^{3+} ions into strontium germanate resulted in a slight shrinkage of the lattice constants and the unit cell volume because Eu^{3+} and Tb^{3+} had smaller radii than Sr^{2+}, indicating the Eu^{3+} and Tb^{3+} ions had been incorporated into the host lattice of $SrGe_4O_9$ and did not change the crystal structure [24]. Those results also suggested that the Eu^{3+} ions substituted into the sites of Sr^{2+} ions. The 2θ value of the (220) diffraction peak was shifted to a higher value, as the concentration of Eu^{3+} was equal to, or greater than, 0.02. The ion radius of Sr^{2+} is 0.130 nm and the ion radius of Eu^{3+} is 0.1087 nm. Hence, as more Sr^{2+} would have been substituted by Eu^{3+}, the ionic radius of the $Sr_{2-x}Eu_xZnMoO_6$ phosphors would have decreased, increasing the 2θ value of the (220) diffraction peak. The ion radius of Eu^{2+} is 0.131 nm, which is thought to be the same as the ion radius of Sr^{2+}. If Eu_2O_3 exists as Eu^{2+} ions, the cell parameters of the $Sr_{2-x}Eu_xZnMoO_6$ phosphors would not have been changed. The shift of the (220) diffraction peak to a higher 2θ value or the decrease in the cell parameters can prove that Eu_2O_3 existed in the $Sr_{2-x}Eu_xZnMoO_6$ phosphors and in the Eu^{3+} state.

In order to find the best doping concentration of Eu^{3+}, we synthesized a series of $Sr_{2-x}Eu_xZnMoO_6$ phosphors (x = 0 to 0.12) and measured their emission spectra. The PL emission spectra of $Sr_{2-x}Eu_xZnMoO_6$ powders excited at a wavelength of 350 nm are shown in Figure 3 for the light wavelength range of 400–650 nm. The spectra in Figure 3 show that that all the excitation spectra of $Sr_{2-x}Eu_xZnMoO_6$ phosphors (except the Sr_2ZnMoO_6 powder) consisted of two parts: one broad band in the 400–575 nm region and two sharp peaks located at 597 nm and 616 nm. However, for the Sr_2ZnMoO_6 powder, even when the synthesizing temperature was 1200 °C, the two sharp peaks of $Sr_{2-x}Eu_xZnMoO_6$ phosphors located at 597 nm and 616 nm were not found in the emission spectra. This means that no characteristic peaks were observed in Sr_2ZnMoO_6 powder even when the synthesizing temperature was 1200 °C. Obviously, the broad band in the 400–575 nm region is assignable to the well-known O^2–Mo^{6+} charge transfer band (CTB) [25]. As Eu_2O_3 was substituted for

SrO, the $Sr_{2-x}Eu_xZnMoO_6$ phosphors had the same spectral profile, but with a different concentration of Eu^{3+} ions, the characteristic peaks were observed.

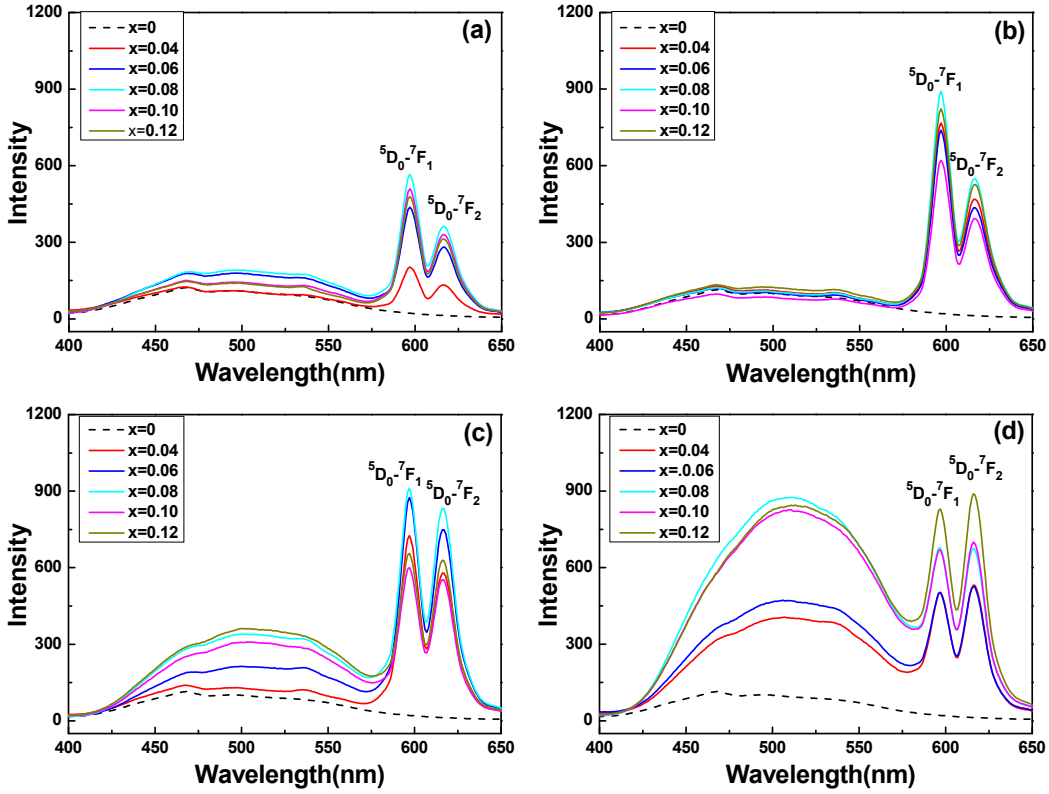

Figure 3. Emission spectra of $Sr_{2-x}Eu_xZnMoO_6$ phosphors synthesized at (**a**) 900 °C; (**b**) 1000 °C; (**c**) 1100 °C; and (**d**) 1200 °C, respectively.

When the synthesizing temperature was changed from 900 to 1200 °C, the emission spectra of the $Sr_{2-x}Eu_xZnMoO_6$ phosphors consisted of sharp peaks in two strong bands at 597 and 616 nm, corresponding to the $^5D_0$–$^7F_1$ (597 nm) and $^5D_0$–$^7F_2$ (616 nm) transitions of Eu^{3+} ions. These results prove that the two emission peaks of the $Sr_{2-x}Eu_xZnMoO_6$ phosphors, $^5D_0$–$^7F_1$ at 597 nm and $^5D_0$–$^7F_2$ at 616 nm, were excited by the addition of Eu^{3+} ions. When the synthesizing temperature was raised to 1100 and 1200 °C, the intensity of the broadened emission went from 400 nm to 575 nm, increasing with the increase in the Eu^{3+} ion concentration. However, the emission intensities of the $Sr_{2-x}Eu_xZnMoO_6$ phosphors were influenced by the synthesizing temperature and the concentration of the Eu^{3+} ions.

In a previous study, the spectra of $BaZrO_3$ doped with Eu^{3+} powders consisted of a series of resolved emission peaks located at 576 nm, 597 nm, 616 nm, 623 nm, 651 nm, 673 nm, 696 nm, and 704 nm, which are assignable to the $^5D_0$–^7F_J (J = 0, 1, 2, 3, 4) transitions of Eu^{3+} ions, namely, $^5D_0$–$^7F_0$ (576 nm), $^5D_0$–$^7F_1$ (597 nm), $^5D_0$–$^7F_2$ (616 nm, 623 nm), $^5D_0$–$^7F_3$ (651 nm), and $^5D_0$–$^7F_4$ (673 nm, 696 nm, and 704 nm) [16]. Liu and Wang's research also showed that the emission intensities of $^5D_0$–$^7F_0$ (576 nm), $^5D_0$–$^7F_1$ (597 nm), and $^5D_0$–$^7F_2$ (616, 623 nm) had almost the same values, even if the Eu concentration in the $BaZr_{1-x}Eu_xO_3$ phosphor powders was different [26]. These previous results [6,16], and the results this study, suggest that the transitions of Eu^{3+} ions between different energy bands are affected by the host materials of the prepared phosphors.

As the synthesizing temperature was changed from 900 °C to 1100 °C, the intensities of the two emission peaks of the $Sr_{2-x}Eu_xZnMoO_6$ phosphors was enhanced by increasing the Eu^{3+} doping concentration and reached a maximum value at x = 0.08. In contrast, the intensities of the two emission peaks of the $Sr_{2-x}Eu_xZnMoO_6$ phosphors decreased when the Eu^{3+} doping ratio was more than 0.08. This proves that the concentration-quenching effect of Eu^{3+} doping happened in the $Sr_{2-x}Eu_xZnMoO_6$

phosphors. When 1200 °C was used as the sintering temperature, the intensities of the two emission peaks of the $Sr_{2-x}Eu_xZnMoO_6$ phosphors increased as the concentration of Eu^{3+} ions rose. The results in Figure 3 also show that when the temperature changed from 1100 °C to 1200 °C, the emission peak varied significantly. For the $Sr_{2-x}Eu_xZnMoO_6$ phosphors, when the synthesizing temperature was changed from 1100 °C to 1300 °C, the emission peak with the maximum intensity shifted from $^5D_0$–$^7F_1$ (597 nm) to $^5D_0$–$^7F_2$ (616 nm). Nevertheless, the strong band at 576 nm corresponding to the $^5D_0$–$^7F_0$ transition was not observed in the emission spectra.

The maximum emission intensities (PL_{max} values) of the $Sr_{2-x}Eu_xZnMoO_6$ phosphors in the transitions of the $^5D_0$–$^7F_1$ (597 nm) and $^5D_0$–$^7F_2$ (616 nm) peaks are presented in Figure 4 as a function of the synthesizing temperature and Eu^{3+} ion concentration. Those results suggest again that the PL characteristics of the $Sr_{2-x}Eu_xZnMoO_6$ phosphors were strongly affected by the synthesizing temperature and the concentration of Eu^{3+} ions. As the x value of the $Sr_{2-x}Eu_xZnMoO_6$ phosphors was smaller than 0.10, the emission intensities of the $^5D_0$–$^7F_1$ (597 nm) and $^5D_0$–$^7F_2$ (616 nm) peaks first increased, reached a maximum, and then decreased as the synthesizing temperature increased. When the x values of $Sr_{2-x}Eu_xZnMoO_6$ phosphors were 0.10 and 0.12, the emission intensity of the $^5D_0$–$^7F_1$ (597 nm) first increased, then decreased at 1100 °C, and then increased at 1200 °C. The emission intensity of the $^5D_0$–$^7F_2$ (616 nm) peaks increased with the increase in synthesizing temperature. These results suggest that 1100 °C is an important synthesizing temperature for $Sr_{2-x}Eu_xZnMoO_6$ phosphors because the transition of PL properties happens at this temperature, but the reasons for this are not known.

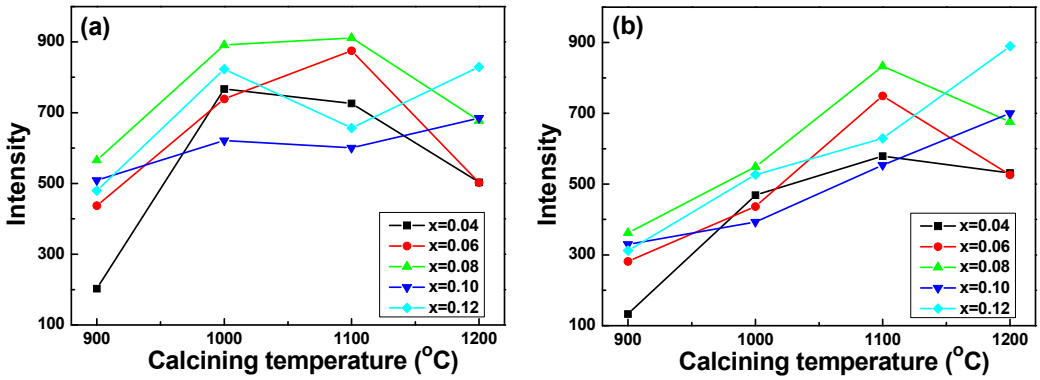

Figure 4. Emission intensity of $Sr_{2-x}Eu_xZnMoO_6$ phosphors as a function of synthesizing temperature. (**a**) Emission peak of 597 nm; and (**b**) emission peak of 616 nm.

The results in Figures 3 and 4 present an important result regarding $Sr_{2-x}Eu_xZnMoO_6$ phosphors: the PL_{max} values of the transition of the $^5D_0$–$^7F_1$ (597 nm) critically increased as the synthesizing temperature increased from 900 °C to 1000 °C, then they did not apparently increase as the synthesizing temperature increased from 1000 °C to 1100 °C, as Figure 4a shows. However, for $Sr_{2-x}Eu_xZnMoO_6$ phosphors with x = 0.04, 0.06, and 0.08, the PL_{max} values of the transition of the $^5D_0$–$^7F_2$ (616 nm) linearly increased as the synthesizing temperature increased from 900 °C to 1100 °C. For $Sr_{2-x}Eu_xZnMoO_6$ phosphors with x = 0.10 and 0.12, the PL_{max} values of the transition of the $^5D_0$–$^7F_2$ (616 nm) linearly increased as the synthesizing temperature increased from 900 °C to 1200 °C, as Figure 4b shows. When the synthesizing temperature was 1200 °C, the emission intensity of the transition of $^5D_0$–$^7F_2$ (616 nm) for $Sr_{1.9}Eu_{0.1}ZnMoO_6$ and $Sr_{1.88}Eu_{0.12}ZnMoO_6$ phosphors was higher than that of $^5D_0$–$^7F_1$ (597 nm), as Figure 4 shows.

The transitions of $^5D_0$–$^7F_1$ (588 nm), $^5D_0$–$^7F_2$ (612 nm), $^5D_0$–$^7F_3$ (649 nm), and $^5D_0$–$^7F_4$ (695 nm) for the Eu^{3+} ions can be simultaneously observed in the emission spectrum of the Eu^{3+}, Tb^{3+}-co-doped one-dimensional strontium germinate, full-color nano-phosphors [24]. However, introduction of the Eu^{3+} ions in the $Sr_{2-x}Eu_xZnMoO_6$ lattice results in disorder. The disorder in the structure will cause transitions in $^5D_0$–$^7F_2$ and point defects in the lattice because of differences in the chemical valence

and in the ionic radius between Eu^{3+} ions and Sr^{2+} ions. The Eu^{3+} ions could occupy either of the sites of Sr^{2+} or the sites of Zn^{2+} (Mo^{2+}) in the $Sr_{2-x}Eu_xZnMoO_6$ phosphor's double-perovskite structure. If Eu^{3+} ions occupy a lattice site with a strict center of symmetry, the odd terms of the static crystal field vanish. This will lead to electric dipole transitions being strictly forbidden for purely electric transitions and the transitions of the $^5D_0$–$^7F_1$ (597 nm) will predominantly produce the emission.

The Eu^{3+} ions could occupy either the tetrahedral sites of Sr^{2+} or the octahedral sites of Zn^{2+} or Mo^{6+} in the $Sr_{2-x}Eu_xZnMoO_6$ double-perovskite crystal structure. Consequently, as both of these sites are centrosymmetric, electric dipole transitions ($^5D_0$–$^7F_{j=0,2}$, only the $^5D_0$–$^7F_2$ transition is observed in this study) are forbidden and, as such, should not appear in the spectra. As the synthesizing temperature is 900 °C, the fact that the $^5D_0$–$^7F_2$ electric dipole transition at 615 nm prevails over the $^5D_0$–$^7F_1$ magnetic dipole transition at 595 nm in the case of $Sr_{2-x}Eu_xZnMoO_6$ phosphors leads us to the conclusion that the Eu^{3+} ions are generally located in a disordered manner in the $Sr_{2-x}Eu_xZnMoO_6$ powders [27]. The charge-compensating oxygen vacancies surrounding the Eu^{3+} ions will lead to the deviation from the point symmetry and relaxation of electric dipole transitions selection rules, with the appearance of the $^5D_0$–$^7F_2$ transition lines in the spectra [27]. Additionally, the Eu^{3+} luminescent centers contributing to the $^5D_0$–$^7F_2$ transition line are probably located at the $Sr_{2-x}Eu_xZnMoO_6$ particle surface or subsurface and will dominate the emission of $Sr_{2-x}Eu_xZnMoO_6$ phosphors when the synthesizing temperature is 1200 °C [27]. If Eu^{3+} ions occupy a non-centrosymmetric lattice site, both electric and magnetic transitions are possible, and the non-symmetric site occupancy will be a dominant reason for causing the emission of $^5D_0$–$^7F_2$ (612 nm) transition [28].

The definition of fluorescence (or phosphorescence) lifetime is the time for the intensity of a single emission peak to decrease to 1/e (approximately 37%) of its original intensity. The decay curves of $Sr_{2-x}Eu_xZnMoO_6$ phosphors were obtained at different concentrations of Eu^{3+} (x = 0.04, 0.06, 0.08, 0.010, and 0.12), and Figure 5 shows the intensity decay of the luminescence of $Sr_{2-x}Eu_xZnMoO_6$ phosphors as a function of the synthesizing temperature, which can be used to calculate the lifetime. The wavelength of the exciting light was 271 nm, and the measured wavelength for the intensity decay was 597 nm ($^5D_0$–$^7F_1$), because it had the maximum emission intensity, as the synthesizing temperature was 900–1100 °C. Typically, the standard form of the single exponential decay function is:

$$A(t) = A_0 \exp[-(t/\tau)] \quad (1)$$

where A_0 is the initial population, τ is constant for the decay time , and t is time. Figure 5 shows that the all curves of decay time can be fitted well by a single-exponential function. Figure 5 also shows that if the same synthesizing temperature is used, the observed decay time is almost unchanged even the x value in $Sr_{2-x}Eu_xZnMoO_6$ phosphor increases from 0.04 to 0.12. Moreover, the decay time is a single exponential function for $Sr_{2-x}Eu_xZnMoO_6$ phosphors with different concentrations of Eu^{3+} ions and synthesized at different temperatures, because the activator lies in the same coordination environment [29].

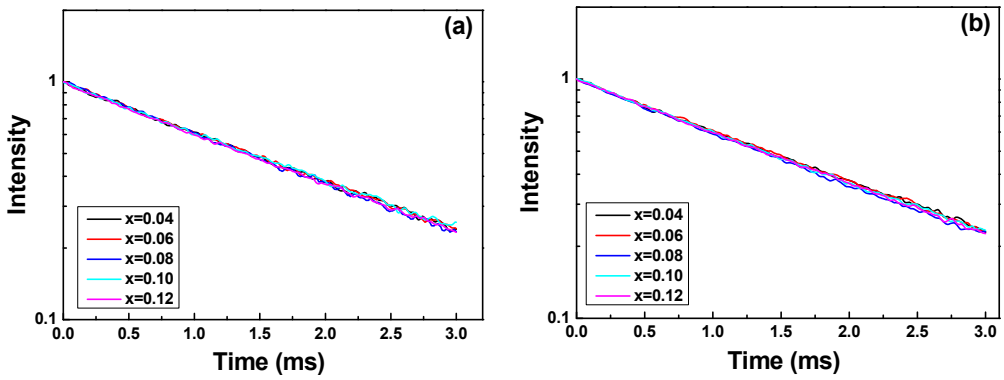

Figure 5. *Cont.*

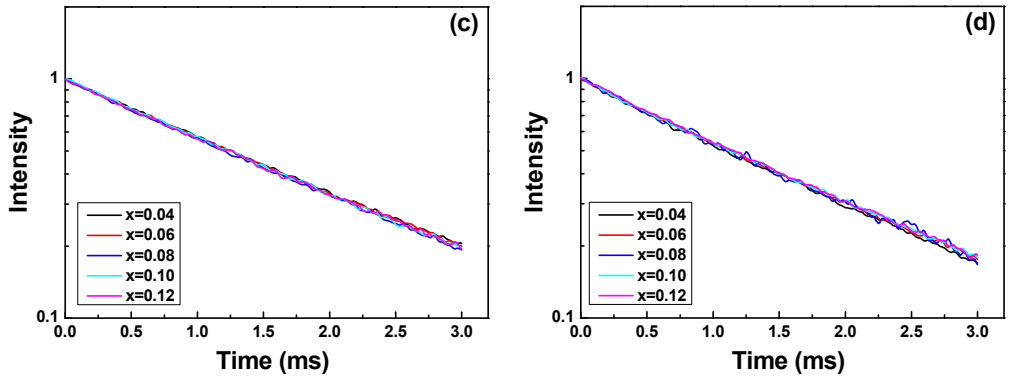

Figure 5. Luminescence lifetime of $Sr_{2-x}Eu_xZnMoO_6$ phosphors synthesized at (**a**) 900 °C; (**b**) 1000 °C; (**c**) 1100 °C; and (**d**) 1200 °C, respectively.

From the results shown in Figure 5, the lifetimes of $Sr_{2-x}Eu_xZnMoO_6$ phosphors, which are compared in Table 1, were measured at 2.04–2.10 ms, 1.93–2.03 ms, 1.78–1.82 ms, and 1.65–1.67 ms, when the synthesizing temperature was 900 °C, 1000 °C, 1100 °C, and 1200 °C, respectively. The lifetimes of $Sr_{2-x}Eu_xZnMoO_6$ phosphors apparently decreased with the increase in the synthesizing temperature. When the synthesizing temperature was 900 °C and 1000 °C, the lifetimes of the $Sr_{2-x}Eu_xZnMoO_6$ phosphors varied more. When the synthesizing temperature was 1100 °C and 1200 °C, the $Sr_{2-x}Eu_xZnMoO_6$ phosphors had less variation in their lifetimes. In Figure 6 we use a fitting curve to find the relationship between lifetime and synthesizing temperature; the equation is:

$$t = -0.0016 \times T + 3.543 \quad (2)$$

where t represents the emitting lifetime of the luminescent material and T represents the synthesizing temperature (°C). In other words, the luminescence lifetime of $Sr_{2-x}Eu_xZnMoO_6$ phosphors can be obtained by using Equation (2), as the synthesizing temperature is changed from 900 °C to 1200 °C. These results suggest that the luminescence lifetime of $Sr_{2-x}Eu_xZnMoO_6$ phosphors can be a function of synthesizing temperature, and that the concentration of Eu^{3+} ions not only can affect their emitting intensity but also can affect their luminescence lifetime.

Table 1. Luminescence lifetimes of $Sr_{2-x}Eu_xZnMoO_6$ phosphors as a function of the synthesizing temperature and concentration of Eu^{3+} ions.

Synthesizing Temperature	X = 0.04	X = 0.06	X = 0.08	X = 0.10	X = 0.12
900 °C	2.05	2.1	2.04	2.04	2.05
1000 °C	2.03	2.03	1.93	1.97	1.99
1100 °C	1.81	1.83	1.78	1.82	1.82
1200 °C	1.65	1.65	1.66	1.66	1.67

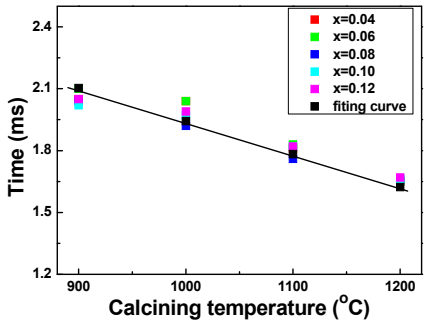

Figure 6. Fitting curve of lifetime for $Sr_{2-x}Eu_xZnMoO_6$ phosphors as a function of the synthesizing temperature and concentration of Eu^{3+} ions.

4. Conclusions

For $Sr_{2-x}Eu_xZnMoO_6$ powders, the 2θ value of the (220) diffraction peak shifted to a higher value and the FWHM value for the (220) diffraction peak decreased as the synthesizing temperature increased. When the x value (the concentration of Eu^{3+} ions) increased from 0 to 0.12 and the synthesizing temperatures rose from 900 °C to 1200 °C, the cell parameters of the $Sr_{2-x}Eu_xZnMoO_6$ powders were changed from $a = b = c/\sqrt{2} = 0.3968$ nm to $a = b = c/\sqrt{2} = 0.3971$ nm and from $a = b = c/\sqrt{2} = 0.3971$ nm to $a = b = c/\sqrt{2} = 0.3974$ nm (cubic crystal structure). When the synthesizing temperature was 900–1100 °C, the emission intensities of the $Sr_{2-x}Eu_xZnMoO_6$ phosphors peaked at $x = 0.08$ and decreased as the concentration of Eu^{+3} ions increased. There was an observable concentration-quenching effect of Eu^{3+} ions in the $Sr_{2-x}Eu_xZnMoO_6$ phosphors. The emission spectrum of Sr_2ZnMoO_6 powder consisted of one broad band in the 400–575 nm region, and the emission spectra of the $Sr_{2-x}Eu_xZnMoO_6$ phosphors (except for the Sr_2ZnMoO_6 powder) consisted of two parts: one broad band in the 400–575 nm region and two sharp peaks located at 597 nm and 616 nm. The lifetimes of the $Sr_{2-x}Eu_xZnMoO_6$ phosphors, which depended on synthesizing temperature and were independent of the concentration of Eu^{3+} ions, were 2.04–2.10 ms, 1.93–2.03 ms, 1.78–1.82 ms, and 1.65–1.67 ms when the synthesizing temperature was 900 °C, 1000 °C, 1100 °C, and 1200 °C, respectively. We found that when the synthesizing temperature was in the range of 900–1200 °C, the relationship between the lifetime and the synthesizing temperature could be determined by the following equation: $t = -0.0016 \times T + 3.543$, where t and T represent the emitting lifetime of the luminescent material and the synthesizing temperature (°C).

Acknowledgments: The authors would like to acknowledge the financial supports of MOST 104-2221-E-390-013-MY2, MOST 105-2622-E-390-003-CC3, and MOST 105-2221-E-344-002.

Author Contributions: S.-H.Y. and J.-L.L. helped proceeding the experimental processes, measurements, and data analysis; C.-Y.L. and C.-F.Y. organized the paper and encouraged in paper writing; Also, C.-Y.L. and C.-F.Y. helped proceeding the experimental processes and measurements.

Conflicts of Interest: The authors declare no conflict of interest.

References

1. Binnemans, K.; Görller-Walrand, C. On the color of the trivalent lanthanide ions. *Chem. Phys. Lett.* **1995**, *235*, 163–174. [CrossRef]
2. Dorenbos, P. The 5d level of positions of the trivalent lanthanides in inorganic compounds. *J. Lumin.* **2000**, *91*, 155–176. [CrossRef]
3. Reid, M.F.; Pieterson, L.V.; Meijerink, A. Trends in parameters for $4f^N \leftrightarrow 4f^{N-1}5d$ spectra of lanthanide ions in crystals. *J. Alloys Compd.* **2002**, *344*, 240–245. [CrossRef]
4. Dorenbos, P. Energy of the first $4f^7 \leftrightarrow 4f^6 5d$ transition of Eu^{2+} in inorganic compounds. *J. Lumin.* **2003**, *104*, 239–260. [CrossRef]
5. Anderson, M.T.; Greenwood, K.B.; Taylor, G.A.; Poeppelmeier, K.R. B-cation arrangements in double perovskites. *Prog. Solid State Chem.* **1993**, *22*, 197–233. [CrossRef]
6. Sivakumar, V.; Varadaraju, U.V. A Promising Orange-Red Phosphor Under Near UV Excitation. *Electrochem. Solid-State Lett.* **2006**, *9*, H35–H38. [CrossRef]
7. Bonilla, C.M.; Landinez Tellez, D.A.; Arbey Rodriguez, J.; Vera Lopez, E.; Roa-Rojas, J. Half-metallic behavior and electronic structure of Sr_2CrMoO_6 magnetic system. *Physica B* **2007**, *398*, 208–211. [CrossRef]
8. Kobayashi, K.-I.; Kimura, T.; Sawada, H.; Terakura, K.; Tokura, Y. Room-temperature magnetoresistance in an oxide material with an ordered double-perovskite structure. *Nature* **1998**, *395*, 677–680. [CrossRef]
9. Yin, H.Q.; Zhou, J.-S.; Zhou, J.-P.; Dass, R.; McDevitt, J.T.; Goodenough, J.B. Intra-versus intergranular low-field magnetoresistance of Sr_2FeMoO_6 thin films. *Appl. Phys. Lett.* **1999**, *75*, 2812–2814. [CrossRef]
10. Jalili, H.; Heinig, N.F.; Leung, K.T. Growth evolution of laser-ablated Sr_2FeMoO_6 nanostructured films: Effects of substrate-induced strain on the surface morphology and film quality. *J. Chem. Phys.* **2010**, *132*, 204701. [CrossRef] [PubMed]
11. Makishima, S.; Yamamoto, H.; Tomotsu, T.; Shionoya, S.J. Luminescence spectra of Sm^{3+} $BaTiO_3$ host lattice. *J. Phys. Soc. Jpn.* **1965**, *20*, 2147–2151. [CrossRef]

12. Li, Y.; Liu, X. Sol–gel synthesis, structure and luminescence properties of Ba_2ZnMoO_6:Eu^{3+} phosphors. *Mater. Res. Bull.* **2015**, *64*, 88–92. [CrossRef]
13. Sivakumar, V.; Varadaraju, U.V. Synthesis, phase transition and photoluminescence studies on Eu^{3+}-substituted double perovskites—A novel orange-red phosphor for solid-state lighting. *J. Solid State Chem.* **2008**, *181*, 3344–3351. [CrossRef]
14. Sivakumar, V.; Varadaraju, U.V. An orange-red phosphor under near-UV excitation for white light emitting diodes. *J. Electrochem. Soc.* **2007**, *154*, J28–J31. [CrossRef]
15. Ye, S.; Wang, C.H.; Liu, Z.S.; Lu, J.; Jing, X.P. Photoluminescence and energy transfer of phosphor series $Ba_{2-z}SrzCaMo_{1-y}WyO_6$:Eu,Li, Li for white light UV LED applications. *Appl. Phys. B* **2008**, *91*, 551–557. [CrossRef]
16. Chen, K.N.; Hsu, C.M.; Liu, J.; Chiu, Y.T.; Yang, C.F. Effect of Different Heating Process on the Photoluminescence Properties of Perovskite Eu-Doped $BaZrO_3$ Powder. *Appl. Sci.* **2016**, *6*, 22. [CrossRef]
17. Li, S.; Wei, X.; Deng, K.; Tian, X.; Qin, Y.; Chen, Y.; Yin, M. A new red-emitting phosphor of Eu^{3+}-doped $Sr_2MgMo_xW_{1-x}O6$ for solid state lighting. *Curr. Appl. Phys.* **2013**, *13*, 1288–1291. [CrossRef]
18. Ye, S.; Wang, C.H.; Jing, X.P. Photoluminescence and Raman Spectra of Double-Perovskite $Sr_2Ca(Mo/W)O_6$ with A- and B-Site Substitutions of Eu^{3+}. *J. Electrochem. Soc.* **2008**, *155*, J148–J151. [CrossRef]
19. Zhang, L.; Lu, J.J.; Liu, J.Q.; Li, Y.; Wang, L.X.; Zhang, Q.T. Structure and luminescent properties of Eu^{3+} doped double perovskite Sr_2CaMoO_6 orange-red phosphors. *Chin. J. Inorg. Chem.* **2012**, *28*, 2036–2042.
20. Ye, S.; Li, Y.; Yu, D.; Yang, Z.; Zhang, Q. Structural effects on Stokes and anti-Stokes luminescence of double-perovskite $(Ba,Sr)_2CaMoO_6$:Yb^{3+},Eu^{3+}. *J. Appl. Phys.* **2011**, *110*, 013517. [CrossRef]
21. Zhang, L.; Han, P.; Han, Y.; Lu, Z.; Yang, H.; Wang, L.; Zhang, Q. Structure evolution and tunable luminescence of $(Sr_{0.98-m}Ba_mEu_{0.02})_2Ca(Mo_{1-n}W_n)O_6$ phosphor with ultraviolet excitation for white LEDs. *J. Alloys Compd.* **2013**, *558*, 229–235. [CrossRef]
22. Wang, Z.J.; Li, P.L.; Yang, Z.P.; Guo, Q.L. Luminescence and concentration quenching of Tb^{3+} in Sr_2ZnMoO_6. *Opt. Commun.* **2014**, *321*, 100–103. [CrossRef]
23. Liu, Y.P.; Chen, S.H.; Fuh, H.R.; Wang, Y.K. First-Principle Calculations of Half-Metallic Double Perovskite $La_2BB'O_6$ (*B*,*B*′ = 3*d* transition metal). *Commun. Comput. Phys.* **2013**, *14*, 174–185. [CrossRef]
24. Lin, L.; Sun, X.; Jiang, Y.; He, Y. Sol-hydrothermal synthesis and optical properties of Eu^{3+}, Tb^{3+}-codoped one-dimensional strontium germanate full color nano-phosphors. *Nanoscale* **2013**, *5*, 12518–12531. [CrossRef] [PubMed]
25. Li, L.; Shen, J.; Pan, Y.; Zhou, X.; Huang, H.; Chang, W.; Ha, Q.; Wei, X. Enhancing luminescence of Lu_2MoO_6:Eu^{3+} phosphors by doping with Li^+ ions for near ultraviolet based solid state lighting. *Mater. Res. Bull.* **2016**, *78*, 26–30. [CrossRef]
26. Liu, X.; Wang, X. Preparation and luminescence properties of $BaZrO_3$:Eu phosphor powders. *Opt. Mater.* **2007**, *30*, 626–629. [CrossRef]
27. Dimitrievska, M.; Ivetic, T.B.; Litvinchuk, A.P.; Fairbrother, A.; Bojan, B.; Miljevic, B.B.; Strbac, G.R.; Rodríguez, A.P.; Lukic-Petrovic, S.R. Eu^{3+}-Doped Wide Band Gap Zn_2SnO_4 Semiconductor Nanoparticles: Structure and Luminescence. *J. Phys. Chem. C* **2016**, *120*, 18887–18894. [CrossRef]
28. Blasse, G.; Bril, A.; Nieuwpoort, W.C. On the Eu^{3+} Fluorescence in Mixed Metal Oxides. *J. Phys. Chem. Solids* **1966**, *27*, 1587–1592. [CrossRef]
29. Xie, A.; Yuan, X.M.; Wang, F.X.; Shi, Y.; Li, J.; Liu, L.; Mu, Z.F. Synthesis and luminescent properties of Eu^{3+}-activated molybdate-based novel red-emitting phosphors for white LEDs. *J. Alloys Compd.* **2010**, *501*, 124–129. [CrossRef]